UPPSALA
UNIVERSITET

On discontinuous Galerkin multiscale methods

Daniel Elfverson
daniel.elfverson@it.uu.se

Division of Scientific Computing
Uppsala University
Sweden

Outline

List of papers

I D. Elfverson and A. Målqvist. *Finite Element Multiscale Methods for Possion's Equation with Rapidly Varying Heterogeneous Coefficients.* In Proc. 10th World Congress on Computational Mechanics, p 10, International Association for Computational Mechanics, Barcelona, Spain, 2012.

II D. Elfverson, G. H. Georgoulis and A. Målqvist. *An Adaptive Discontinuous Galerkin Multiscale Method for Elliptic Problems.* To appear in Multiscale Modeling and Simulation (MMS).

III D. Elfverson, G. H. Georgoulis, A. Målqvist and D. Peterseim. *Convergence of a Discontinuous Galerkin Multiscale Method.* In review in SIAM Journal on Numerical Analysis (SINUM), available as preprint arXiv:1211.5524, 2012.

IV D. Elfverson and A. Målqvist. *Discontinuous Galerkin Multiscale Methods for Convection Dominated Problems.* Technical Report 2013-011, Department of Information Technology, Uppsala University, 2013.

Main contributions

The main contributions of this thesis are the following:

- The development of a multiscale method, the "Discontinuous Galerkin multiscale method", using the framework for the variational multiscale method and the discontinuous Galerkin method for Poisson's equation with variable coefficients. See Paper I, II, and III.

Main contributions

The main contributions of this thesis are the following:

- The development of a multiscale method, the "Discontinuous Galerkin multiscale method", using the framework for the variational multiscale method and the discontinuous Galerkin method for Poisson's equation with variable coefficients. See Paper I, II, and III.
- A priori error bounds with respect to the coarse mesh size, independent of the variation in data and without any assumption on scale separation or periodicity. See Paper III.

Main contributions

The main contributions of this thesis are the following:

- The development of a multiscale method, the "Discontinuous Galerkin multiscale method", using the framework for the variational multiscale method and the discontinuous Galerkin method for Poisson's equation with variable coefficients. See Paper I, II, and III.
- A priori error bounds with respect to the coarse mesh size, independent of the variation in data and without any assumption on scale separation or periodicity. See Paper III.
- Development of an adaptive algorithm, using a posteriori error bounds, to tune the method parameters in order to get efficient and reliable approximations. See Paper II.

Main contributions

The main contributions of this thesis are the following:

- The development of a multiscale method, the "Discontinuous Galerkin multiscale method", using the framework for the variational multiscale method and the discontinuous Galerkin method for Poisson's equation with variable coefficients. See Paper I, II, and III.
- A priori error bounds with respect to the coarse mesh size, independent of the variation in data and without any assumption on scale separation or periodicity. See Paper III.
- Development of an adaptive algorithm, using a posteriori error bounds, to tune the method parameters in order to get efficient and reliable approximations. See Paper II.
- The development of a multiscale method for convection dominated problems together with a proof of convergence under mild assumptions on the magnitude of the convection term. See Paper IV.

Motivation of discontinuous Galerkin multiscale method

- Computer simulation of problems involving several different scales (multiscale problems) and is one of the greatest challenges in scientific computing today.
- Discontinuous Galerkin method has a good conservation properties of the state variable.
- Non-conforming meshes are admissible.
- The element-wise L^2-projection is admissible as the split between the coarse and fine scale.

Model problem

Consider the PDE

$$-\nabla \cdot A \nabla u = f \text{ in } \Omega,$$
$$u = 0 \text{ on } \partial\Omega.$$

which in weak (variational) form reads: find $u \in \mathcal{V} := H^1_0(\Omega)$ such that

$$a(u,v) := \int_\Omega A \nabla u \cdot \nabla v \, dx = \int_\Omega f v \, dx =: F(v) \quad \text{for all } v \in \mathcal{V},$$

for $0 < A_{min} \in \mathbb{R} \leq A(x) \in L^\infty(\Omega)$ and $f \in L^2(\Omega)$.

Discontinuous Galerkin discretization

- Split Ω into a elements $\mathcal{T} = \{T\}$, and let $\mathcal{E} = \{e\}$ be the set of all edges in $\mathcal{T}$.

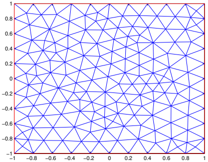

Figure: Example of a mesh on a unit square.

- Let $\mathcal{V}_H$ be the space of all discontinuous piecewise (bi)linear polynomials.

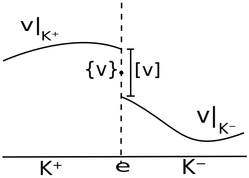

Figure: Example of $\{v\}$ and $[v]$

Let

$$
\begin{aligned}
a_H(v,z) = \sum_{T\in\mathcal{T}} (A\nabla v, \nabla z)_{L^2(T)} - \sum_{e\in\mathcal{E}} \Big((\mathbf{n}\cdot\{A\nabla v\}, [z])_{L^2(e)} \\
+ (\mathbf{n}\cdot\{A\nabla z\}, [v])_{L^2(T)} - \frac{\sigma_e\gamma_e}{H_e}([v],[z])_{L^2(e)} \Big), \\
F(v) = (f, v)_{L^2(\Omega)}.
\end{aligned}
$$

where

$$
|||v|||^2 = \sum_{T\in\mathcal{T}} \|\sqrt{A}\nabla v\|^2_{L^2(T)} + \sum_{e\in\mathcal{E}} \frac{\sigma_e\gamma_e}{H_e}\|[v]\|^2_{L^2(e)}
$$

(One scale) DG method

Find $u_H \in \mathcal{V}_H$ such that

$$
a_H(u_H, v) = F(v), \quad \text{for all } v \in \mathcal{V}_H.
$$

(One scale) DG method

Find $u_H \in \mathcal{V}_H$ such that

$$a_H(u_H, v) = F(v), \quad \text{for all } v \in \mathcal{V}_H.$$

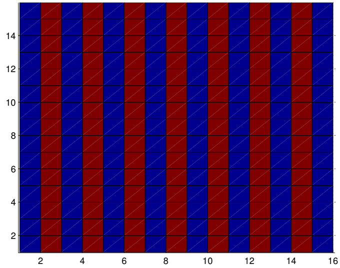

Figure: The coefficient A in the model problem.

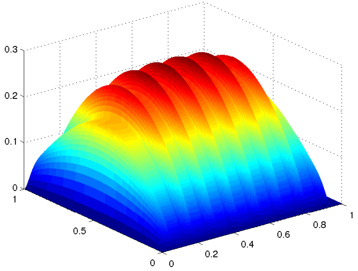

Figure: Reference solution.

(One scale) DG method

Find $u_H \in \mathcal{V}_H$ such that

$$a_H(u_H, v) = F(v), \quad \text{for all } v \in \mathcal{V}_H.$$

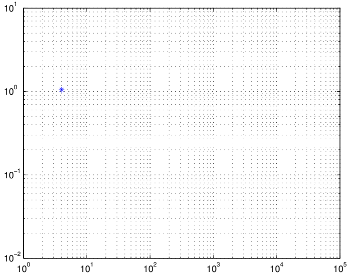

Figure: Energy norm with respect to the degrees of freedom.

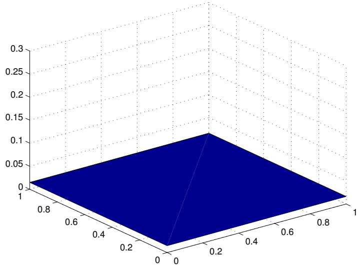

Figure: Solution obtained using the discontinuous Galerkin method.

(One scale) DG method

Find $u_H \in \mathcal{V}_H$ such that

$$a_H(u_H, v) = F(v), \quad \text{for all } v \in \mathcal{V}_H.$$

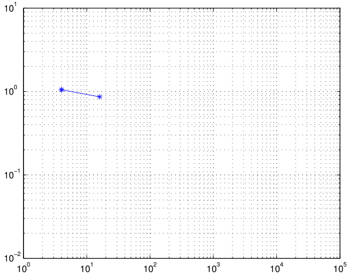

Figure: Energy norm with respect to the degrees of freedom.

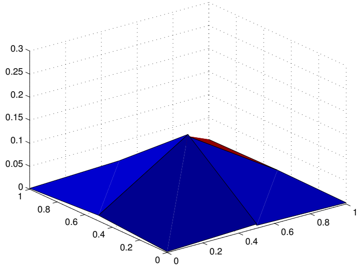

Figure: Solution obtained using the discontinuous Galerkin method.

(One scale) DG method

Find $u_H \in \mathcal{V}_H$ such that

$$a_H(u_H, v) = F(v), \quad \text{for all } v \in \mathcal{V}_H.$$

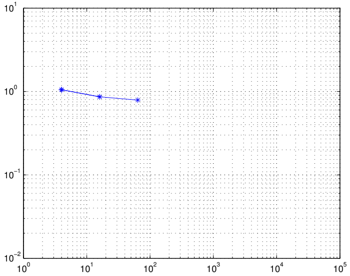

Figure: Energy norm with respect to the degrees of freedom.

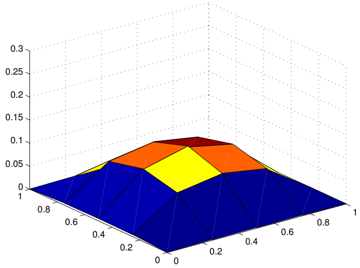

Figure: Solution obtained using the discontinuous Galerkin method.

(One scale) DG method

Find $u_H \in \mathcal{V}_H$ such that

$$a_H(u_H, v) = F(v), \quad \text{for all } v \in \mathcal{V}_H.$$

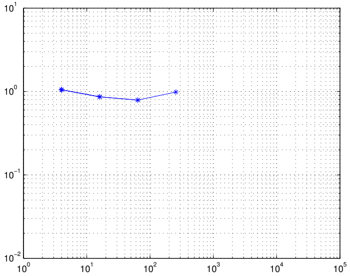

Figure: Energy norm with respect to the degrees of freedom.

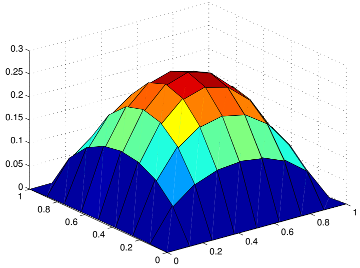

Figure: Solution obtained using the discontinuous Galerkin method.

(One scale) DG method

Find $u_H \in \mathcal{V}_H$ such that

$$a_H(u_H, v) = F(v), \quad \text{for all } v \in \mathcal{V}_H.$$

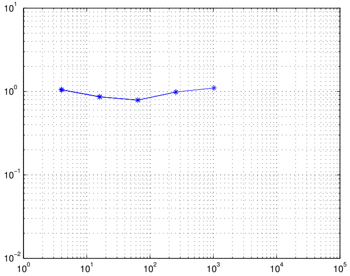

Figure: Energy norm with respect to the degrees of freedom.

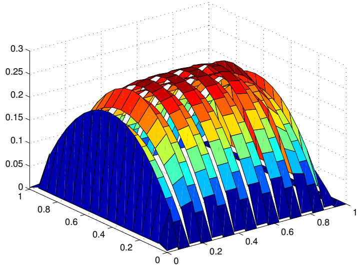

Figure: Solution obtained using the discontinuous Galerkin method.

(One scale) DG method

Find $u_H \in \mathcal{V}_H$ such that

$$a_H(u_H, v) = F(v), \quad \text{for all } v \in \mathcal{V}_H.$$

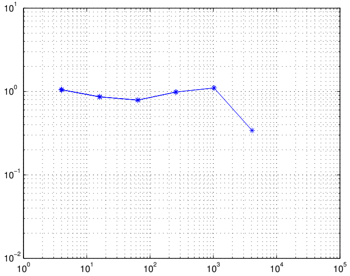

Figure: Energy norm with respect to the degrees of freedom.

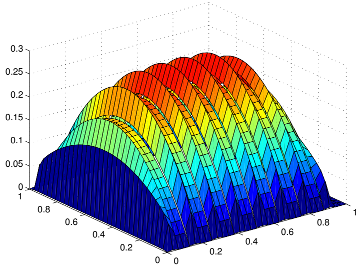

Figure: Solution obtained using the discontinuous Galerkin method.

(One scale) DG method

Find $u_H \in \mathcal{V}_H$ such that

$$a_H(u_H, v) = F(v), \quad \text{for all } v \in \mathcal{V}_H.$$

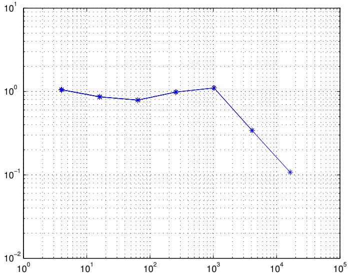

Figure: Energy norm with respect to the degrees of freedom.

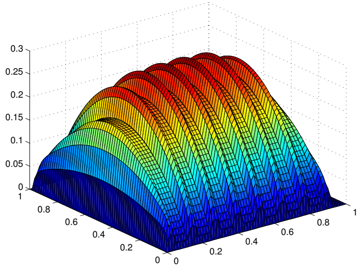

Figure: Solution obtained using the discontinuous Galerkin method.

(One scale) DG method

Find $u_H \in \mathcal{V}_H$ such that

$$a_H(u_H, v) = F(v), \quad \text{for all } v \in \mathcal{V}_H.$$

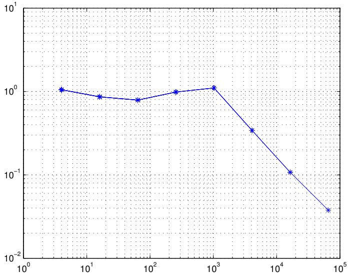

Figure: Energy norm with respect to the degrees of freedom.

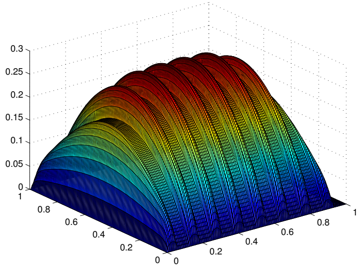

Figure: Solution obtained using the discontinuous Galerkin method.

Objective with the multiscale method

- Eliminate the dependency of A via a multiscale method i.e.,

$$|||u - u_H^{ms,L}||| \leq C_f H,$$

  where H does not resolve the variation in A
- Construct an adaptive algorithm to focus computational effort to critical areas.

Multiscale split

- Consider a coarse $\mathcal{V}_H$ and a fine space $\mathcal{V}_h$, such that $\mathcal{V}_H \subset \mathcal{V}_h$.
- Let Π_H be the L^2-projection onto $\mathcal{V}_H$. This will be used as the split between the coarse and fine scale.
- Define $\mathcal{V}^f(\omega) = \{v \in \mathcal{V}_h(\omega) : \Pi_H v = 0\}$.
- We have a L^2-orthogonal split; $\mathcal{V}_h = \mathcal{V}_H \oplus \mathcal{V}^f$.

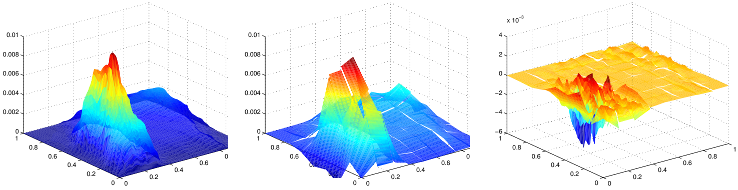

Figure: $u_h = u_H + u^f$

Corrected basis functions

- For each basis function $\lambda_{T,j} \in \mathcal{V}_H$ we calculate a corrector, find $\phi^L_{T,j} \in \mathcal{V}^f(\omega^L_T)$ such that

$$a_h(\phi^L_{T,j}, v_f) = a_h(\lambda_{T,j}, v_f), \quad \text{for all } v_f \in \mathcal{V}^f(\omega^L_T).$$

  where $\text{supp}(\lambda_{T,j}) = T$ and L indicates the size of the patch.
- Let the new corrected space be defined by $\mathcal{V}^{ms}_H = \text{span}\{\lambda_{T,j} - \phi^L_{T,j}\}$.
- We have an a_h-orthogonal split; $\mathcal{V}_h = \mathcal{V}^{ms}_H \oplus \mathcal{V}^f$

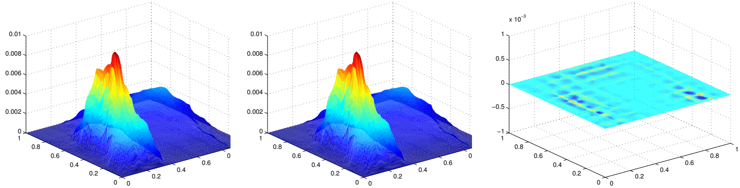

Figure: $u_h = u^{ms}_H + u^f$

Examples of corrected basis functions

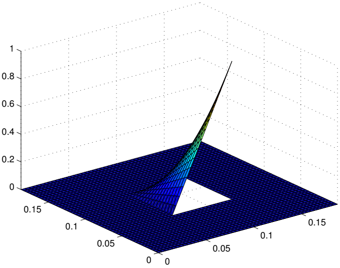

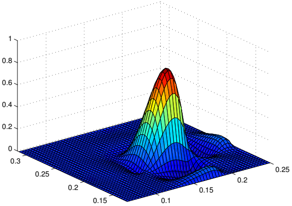

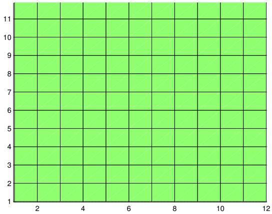

Examples of corrected basis functions

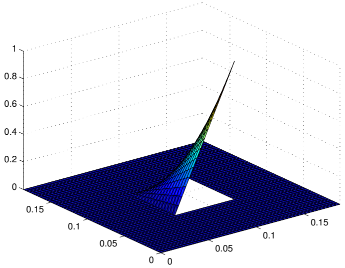

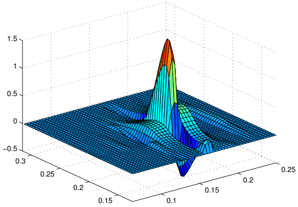

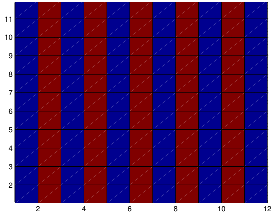

Examples of corrected basis functions

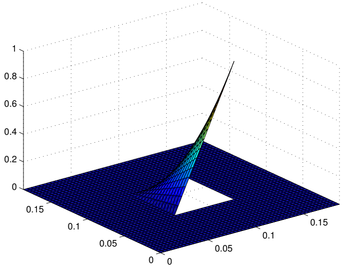

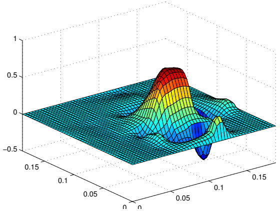

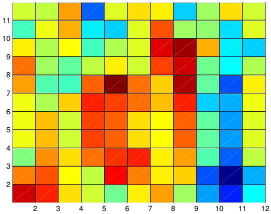

Discontinuous Galerkin multiscale method

Consider the problem: find $u_H^{ms,L} \in \mathcal{V}_L^{ms} = \text{span}\{\lambda_{T,j} - \phi_{T,j}^L\}$ such that

$$a_h(u_H^{ms,L}, v) = F(v), \quad \text{for all } v \in \mathcal{V}_H^{ms,L}.$$

A priori results

Lemma (Decay of corrected basisfunctions)

For $\phi_{T,j} \in \mathcal{V}^f(\omega_i^L)$, there exist a, $0 < \gamma < 1$, such that

$$|||\phi_{T,j} - \phi_{T,j}^L||| \lesssim \gamma^L |||\lambda_j - \phi_{T,j}|||.$$

Theorem

For $u_H^{ms,L} \in \mathcal{V}_H^{ms,L}$, there exist a, $0 < \gamma < 1$, such that

$$|||u - u_H^{ms,L}||| \lesssim |||u - u_h||| + ||H(f - \Pi_H f)||_{L^2} + H^{-1}(L)^{d/2}\gamma^L ||f||_{L^2}.$$

Choosing $L = \lceil C \log(H^{-1}) \rceil$ both terms behave in the same manor with an appropriate C.

Numerical verification

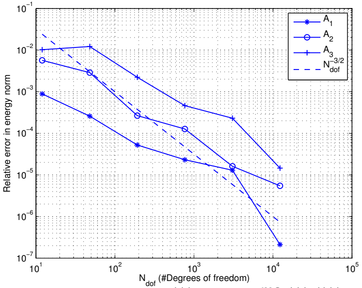

Figure: $\#dofs$ vs $|||u_h - u^{ms}_{H,L}|||/|||u_h|||$

- Choose $L = \lceil 2\log(\frac{1}{H})\rceil$.
- Let the right hand side be: $f = 1 + sin(\pi x) + sin(\pi y)$.
- Let $H = 2^{-m}$ for $m = \{1, 2, 3, 4, 5, 6\}$.
- Reference mesh is 2^{-8}.

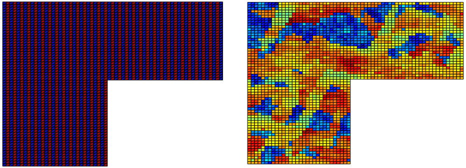

Figure: Permeabilities are piecewise constant on a mesh with size 2^{-5}, with ratio $A_{max}/A_{min} = \{10, 7 \cdot 10^6\}$

Adaptivity and a posteriori error bound

Theorem (A posteriori error bound)

Let $u_H^{ms,L}$ be the multiscale solution, then

$$|||u - u_H^{ms,L}||| \lesssim \left(\sum_{T \in \mathcal{T}_H} \rho_{h,T}^2 \right)^{1/2} + \left(\sum_{T \in \mathcal{T}_H} \rho_{L,\omega_T^L}^2 \right)^{1/2}.$$

- $\rho_{L,\omega_i^L}^2$ and $\rho_{h,K}^2$ depends on $u_H^{ms,L}$
- $\rho_{L,\omega_i^L}^2$ measures the effect of the truncated patches.
- $\rho_{h,T}^2$ measures the effect of the refinement level.

Numerical experiment

- We conider the permeabilities

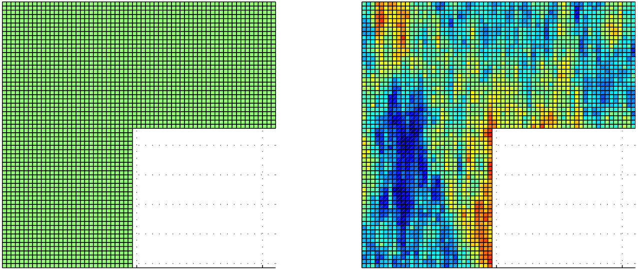

Figure: Permeabilities *One* left and *SPE* right.

Numerical experiments

- Using a refinement level of 30% we have.

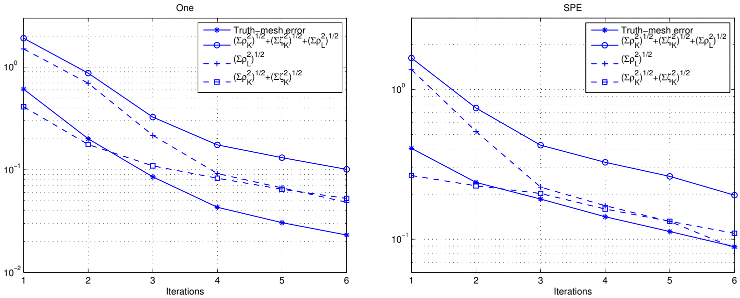

Figure: Convergence plot for *One* left and *SPE* right.

Numerical experiments

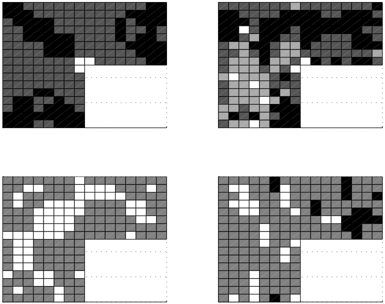

Figure: The level of refinement and size of the patches illustrated in the upper resp. lower plots for the different permeability One (left) and SPE (right). White is where most refinements resp. larger patch are used and black is where least refinements resp. smallest patches are used.

Convection dominated problems

Consider the PDE

$$-\nabla \cdot A \nabla u + \mathbf{b} \cdot \nabla u + cu = f \text{ in } \Omega,$$
$$u = 0 \text{ on } \partial\Omega.$$

A discontinuous Galerkin approximation reads: find $u \in \mathcal{V}_H$ such that

$$a_H(u, v) = F(v) \quad \text{for all } v \in \mathcal{V}_H,$$

where the diffusion term is approximated as earlier and the convective term by upwind.

Convergence results

Under the assumation $\mathcal{O}(\|A\|_{L^\infty(\Omega)}) = \mathcal{O}(\|H\mathbf{b}\|_{L^\infty(\Omega)})$ the following holds:

Lemma (Decay of modifed basisfunction)

For $\phi_{T,j} \in \mathcal{V}^f(\omega_i^L)$, there exist a, $0 < \gamma < 1$, such that

$$|||\phi_{T,j} - \phi_{T,j}^L||| \lesssim \gamma^L |||\lambda_j - \phi_{T,j}|||.$$

Theorem

For $u_H^{ms,L} \in \mathcal{V}_H^{ms,L}$, there exist a, $0 < \gamma < 1$, such that

$$|||u - u_H^{ms,L}||| \lesssim |||u - u_h||| + ||H(f - \Pi_H f)||_{L^2} + H^{-1}(L)^{d/2}\gamma^L ||f||_{L^2}.$$

Choosing $L = \lceil C \log(H^{-1}) \rceil$ both terms behave in the same manor with an appropriate C.

Example of corrected basisfunction

- With $\mathbf{b} = [0, 0]'$.

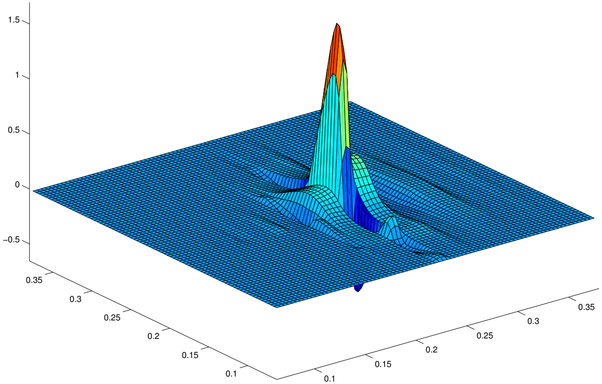

Example of corrected basisfunction

- With $\mathbf{b} = -[1, 0]'$.

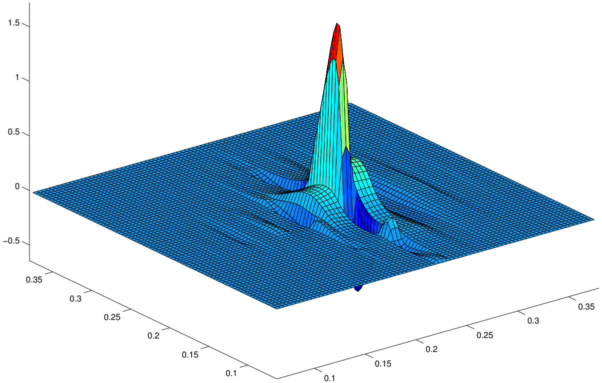

Example of corrected basisfunction

- With $\mathbf{b} = -[2, 0]'$.

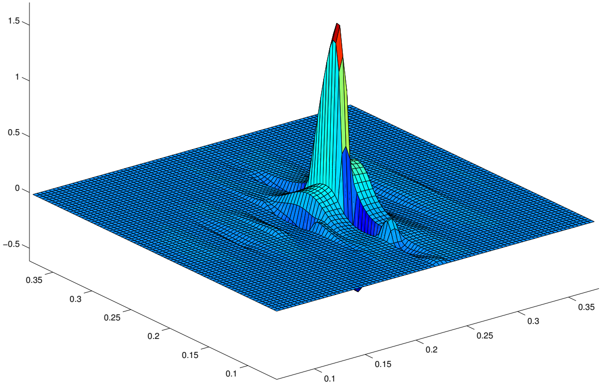

Example of corrected basisfunction

- With $\mathbf{b} = -[4,0]'$.

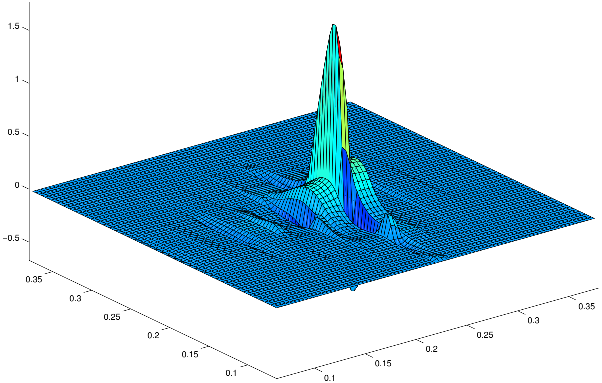

Example of corrected basisfunction

- With $\mathbf{b} = [8, 0]'$.

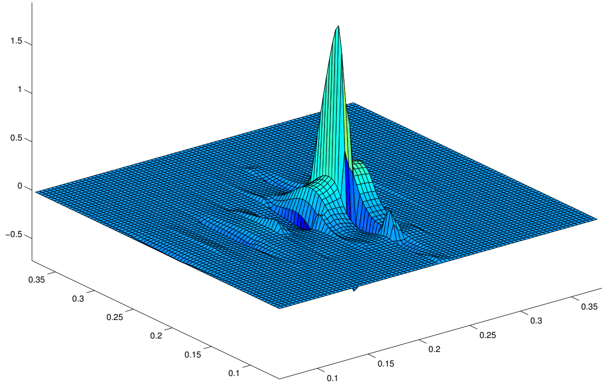

Example of corrected basisfunction

- With $\mathbf{b} = -[16, 0]'$.

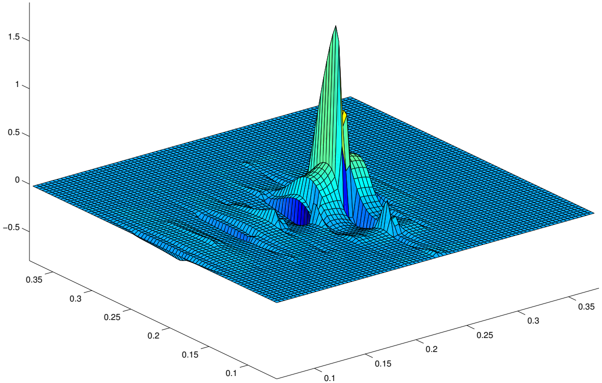

Numerical verification

$$-\nabla \cdot A\nabla u + \mathbf{b} \cdot \nabla u + cu = f \text{ in } \Omega,$$
$$u = 0 \text{ on } \partial\Omega.$$

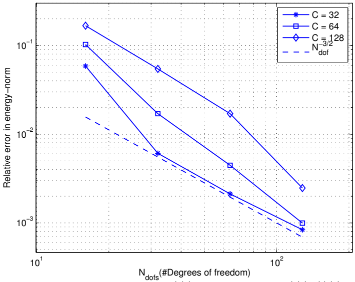

Figure: $\#dofs$ vs $|||u_h - u_{H,L}^{ms}|||/|||u_h|||$

- Let $A = 1$, $c = 0$, and $\mathbf{b} = C[1,0]'$ for $C = 32, 54, 128$.
- Choose $L = \lceil 2\log(\frac{1}{H}) \rceil$.
- Let the right hand side be: $f = 1 + sin(\pi x) + sin(\pi y)$.
- Let $H = 2^{-m}$ for $m = \{2, 3, 4, 5\}$.
- Reference mesh is 2^{-7}.

$$-\nabla \cdot A\nabla u + \mathbf{b} \cdot \nabla u + cu = f \text{ in } \Omega,$$
$$u = 0 \text{ on } \partial\Omega.$$

- Let $c = 0$, and $\mathbf{b} = [1, 0]'$.

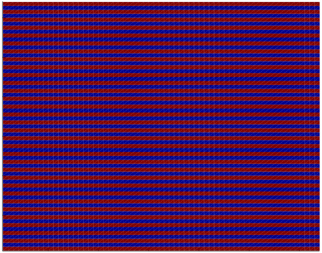

Figure: Diffusion coefficent A, $A_{max}/A_{min} = 0.01$.

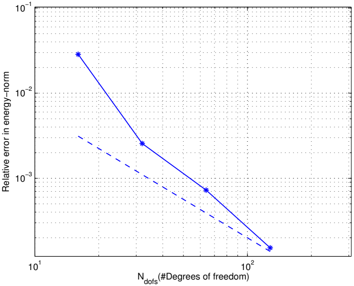

Figure: $\#dofs$ vs $|||u_h - u^{ms}_{H,L}|||/|||u_h|||$

$$-\nabla \cdot A\nabla u + \mathbf{b} \cdot \nabla u + cu = f \text{ in } \Omega,$$
$$u = 0 \text{ on } \partial\Omega.$$

- Let $c = 0$, and $\mathbf{b} = [512, 0]'$.

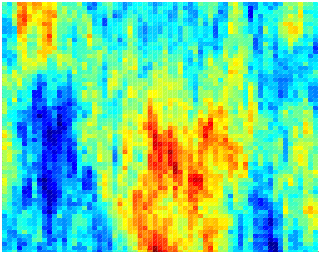

Figure: Diffusion coefficent A.

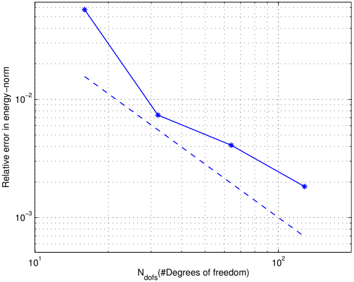

Figure: $\#dofs$ vs $|||u_h - u^{ms}_{H,L}|||/|||u_h|||$

Paper I

D. Elfverson and A. Målqvist. *Finite Element Multiscale Methods for Possion's Equation with Rapidly Varying Heterogeneous Coefficients.* In Proc. 10th World Congress on Computational Mechanics, p 10, International Association for Computational Mechanics, Barcelona, Spain, 2012.

An abstract framework for constructing finite element multiscale methods based on the VMS is presented. Using this framework we propose and compare two different multiscale methods, one based on the continuous Galerkin finite element method and one on the discontinuous Galerkin finite element method. The continuous Galerkin multiscale method uses local Dirichlet problems and the discontinuous Galerkin multiscale method uses local Neumann problems, for the localized fine scale problems.

Paper II

D. Elfverson, G. H. Georgoulis and A. Målqvist. *An Adaptive Discontinuous Galerkin Multiscale Method for Elliptic Problems.* To appear in Multiscale Modeling and Simulation (MMS).

We present an adaptive discontinuous Galerkin multiscale method driven by an energy norm a posteriori error bound. The a posteriori error bound is used within an adaptive algorithm to tune the critical parameters, i.e., the refinement level and the size of the different patches on which the fine scale constituent problems are solved. We solve local Dirichlet problem instead for Neumann problem (Paper I) for the localized fine scale problems.

Paper III

D. Elfverson, G. H. Georgoulis, A. Målqvist, and D. Peterseim. *Convergence of a Discontinuous Galerkin Multiscale Method.* In review in SIAM Journal on Numerical Analysis (SINUM), available as preprint arXiv:1211.5524, 2012.

A convergence result for a discontinuous Galerkin multiscale method for a second order elliptic problem is presented. We prove that the error, due to truncation of corrected basis, decreases exponentially with the size of the patches. The same corrected basis as in Paper II is used. Improved convergence rate can be achieved depending on the piecewise regularity of the forcing function. Linear convergence in energy norm and quadratic convergence in L^2-norm is obtained independently of the forcing function.

Paper IV

D. Elfverson and A. Målqvist. *Discontinuous Galerkin Multiscale Methods for Convection Dominated Problems.* Technical Report 2013-011, Department of Information Technology, Uppsala University, 2013.

In this paper we extend the discontinuous Galerkin multiscale method in Paper III to convection dominated problems. The advantages of the multiscale method and the discontinuous Galerkin method allows us to better cope with multiscale features and boundary layers in the solution. We prove decay of the corrected basis functions as well as an a priori error bound for the multiscale method.

Future work

There are many aspects in multiscale methods which still are relatively new and open for research. A few examples which would be interesting to investigate further are:

- Construction of an adaptive algorithm which balances the error caused by the uncertainty in the data and the discretization error, which are two important error sources for multiscale problems.
- Implement the methods on parallel machines to allow 3D simulations.
- Consider non-linear convection dominated problems with applications in two-phase flow, where systems of a coupled convection dominated transport equations and elliptic pressure equations arise.

The End